Monte-Carlo Simulations of Light Transmission for the CTOF Light Monitoring System

Gegham Asryan

October 4, 2016

Abstract

Results are presented for Monte-Carlo (*MC*) light transmittance simulations for an Integrating Sphere Light Transmitter (*ISLT*) with an isotropic-diffuse reflecting surface compared to two different designs for Acrylic Light Guides: a) Cylindrical Acrylic Light Guide (*CALG*) and b) Focusing Truncated Conical Acrylic Light Guide ($FTCALG$). These represent three different options for the light transmitter of the Light Monitoring System (*LMS*) of the *CLAS*12 Central Time-of-Flight ($CTOF$) system that couples the input Light Source (*LS*) to the output Fiber Bundle (FB) that connects to the $CTOF$ counters. Also shown are results of calculations using data from the Technical Note of the *ISLT* manufacturer (https://www.labsphere.com/site/assets/files/2551/a-guide-to-integrating-sphere-theory-and-applications.pdf).

An important and basic property of any Light Transmitter is the **Percent of Light Flux** accepted by the exit port area from the input port area (also called the transmittance). In the *LMS* the exit port is coupled to a Fiber Bundle (FB, bundle includes 110 fibers) and the input port is coupled to an LED Light Source (*LS*).

The goals of this *MC* simulation were to define the fraction of the light accepted by the FB in the case of using either the *ISLT*, *CALG*, or $FTCALG$, and then to compare the results. The studies also determined the light pulse propagation time and path length due to the multiple reflections within the *ISLT*.

The isotropic reflecting wall of the *ISLT*, which in the simulation ranges from $-85^\circ \rightarrow 85^\circ$ (close to a 2π sr solid angle), provides for a uniform distribution of light on the *ISLT*'s output window, which is the input of the FB. The *LS* and FB in the *ISLT* are mounted at $\approx 90^\circ$ to each other (see Fig. 1 left). There is a diffuse screen mounted inside the *ISLT* between the *LS* and the FB that prevents direct light from the *LS* from reaching the FB.

Two different lengths for the *CALG* and $FTCALG$ have been studied with radii on both sides a little larger than the *LS* and FB. For the smaller radius of the $FTCALG$ cone (touching the FB), two different radii where used in the simulations in order to optimize the fraction of light reaching the FB. For the larger side (touching the *LS*), the studies of the designs of the two different lengths employed the same radius.

1 *ISLT*, *LS*, and *FB* Setup

The actual dimensions from the manufacturer for the *ISLT* and *FB* were used in the *MC* simulations and are shown in Table 1, together with the radius and the light flux range for the Light Source (*LS*). The *LS* is a JLab design and is shown in Fig. 1 right. The *LS* included six *LED*s located on the perimeter of a disk with a 3.25 mm radius. The angular range of the light flux cone from each *LED* is $\pm 10^{\circ}$ as they are equipped with light focusing lenses.

Integrating Sphere Radius (mm)	50.0
Light Source Radius (mm)	3.25
Fiber Bundle Radius (mm)	5.00
Light Spread Angular Range	$\pm 85^{\circ}$
Light Source Flux Angular Range	$\pm 10^{\circ}$

Table 1: Dimensions of the *ISLT*.

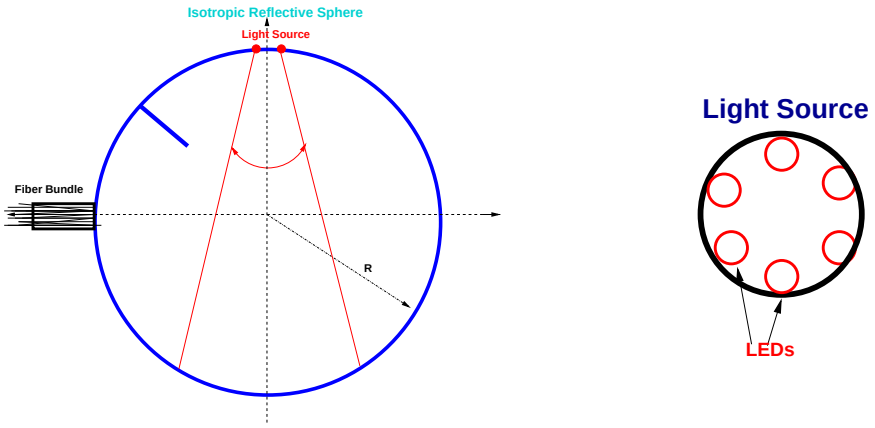

Figure 1: (Left) *ISLT* with the *LS* and *FB* coupled to its input and output ports, respectively. (Right) Schematic of the six *LED* Light Source.

The *ISLT*, as mentioned above, has openings for the *LS* and *FB*. The design of the *ISLT* required the relative positions of the *LS* and *FB* to be at 90° with respect to each other as shown in Fig. 1 left. The *FB* consists of an opaque plastic cylinder harness containing the fiber bundle along its central axis. In the simulation a 5.0 mm radius was used for the fibers. Straight light from the *LS* cannot reach the *FB* due the geometry of the *ISLT* and the angular range of the *LS* light flux.

2 Results of *ISLT* Simulations

The light can reach the *FB* only by multiple reflections from the isotropically-diffuse reflecting surface of the *ISLT*. A sample of several diffuse reflections of light inside the *ISLT* is shown in Fig. 2. If the wall of the *ISLT* has a **Reflectance** ρ, the **Remaining Intensity** of light reaching the *FB* after N_r reflections is Φ_r, where $\Phi_r = \Phi_0 \cdot \rho^{N_r}$. The number of reflections after which the light intensity has decreased to a given **Remaining Intensity** level is given by $N_r = \frac{ln(\frac{\Phi_r}{\Phi_0})}{ln(\rho)}$, where Φ_0 is the initial intensity flux from the *LS*. If $\rho \approx 97\%$ (the value used in the simulation), then Φ_r is $\leq 50\%$ of Φ_0 if $\mathbf{N_r \geq 23}$.

In the *MC* simulation several different values for the number of reflections were used as input parameters, corresponding to different amounts of light intensity reaching the *FB*. The results of the *MC* simulation for light transmission are shown in Table 2 (for various values of $\mathbf{N_r \leq 80}$) and Fig. 3. The *MC* simulation was done for 10 million events for each run for the number of reflections. The total path length of the light for all reflections arriving at the *FB* was calculated, as well as the propagation time for the light at the input to the *FB*, and is shown in Fig. 3.

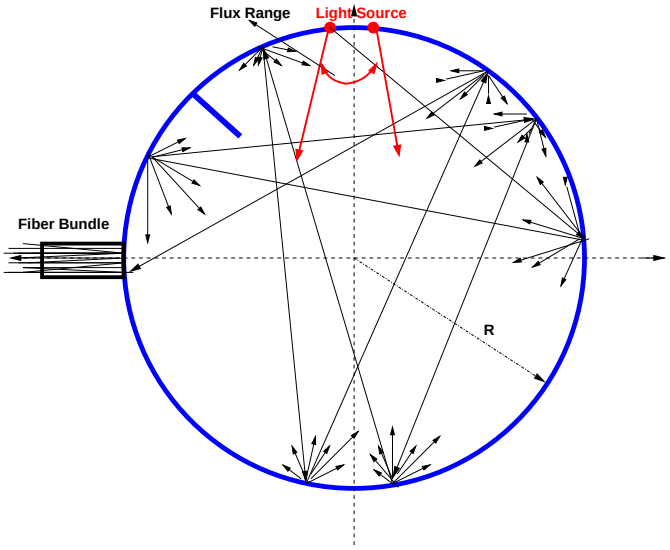

Figure 2: Typical light reflections within the *ISLT*.

Intensity Ratio $\frac{\Phi_r}{\Phi_0}$ (%)	97	89	74	54	30	9
Number of reflections	1	4	10	20	40	80
Accepted by *FB* (%)	0.3	1.0	2.5	4.9	9.5	18.0
Maximum Time (ns)	0.6	1.1	2.2	4.9	8.3	17.0
Maximum Path (mm)	190.0	337.8	672.6	1481.5	2482.6	5091.0

Table 2: Results of simulations for the *ISLT*.

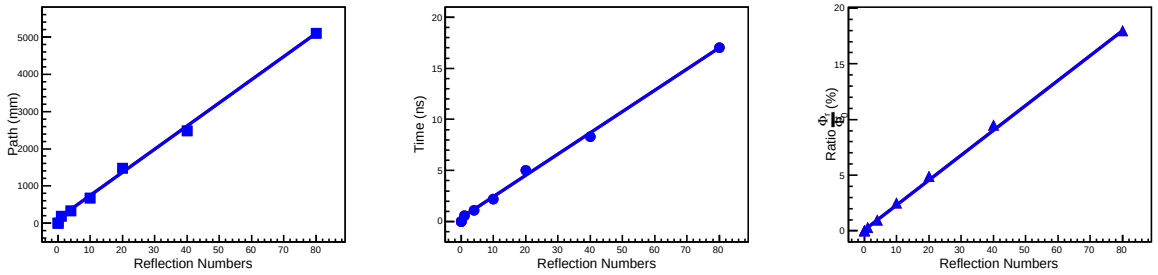

Figure 3: **Light Path Length** (left), **Propagation Time** (center), and **Light Transmission** (right) as a function of the number of reflections in the *ISLT*.

3 *ISLT* Theoretical Calculations

One of the basic parameters of the integrating sphere is its **Reflectance** (ρ). Its other important parameters include:

1. **Port Fraction:** $f = \frac{A_i + A_e}{A_s}$
2. **Exchange Factor:** $F_{i-e} = \frac{A_e}{4 \cdot \pi \cdot R^2} = \frac{A_e}{A_s}$
3. **Multiplicity:** $M = \frac{\rho}{1-\rho \cdot (1-f)}$,

where A_i is the input port area, A_e is the exit port area, and A_s is the inside surface area of the sphere.

The **Port Fraction** (f) is the ratio of the input port area A_i and exit port area A_e relative to the entire sphere surface area A_s.

The **Exchange Factor** F_{i-e} is the fraction of the light flux entering A_i and arriving at A_e. It is same for any radiating point on the sphere surface. In fact, the fraction of the radiant flux received by A_e is the fractional surface area it occupies within the sphere.

The **Multiplicity** (M) strong depends on the Reflectance ρ and the Port Fraction f, and represents the average reflectance $\overline{\rho}$ of the entire integrating sphere.

The Integrating Sphere under study for the *CTOF LMS* has the following parameters: Sphere Radius: 50 mm, radius of port for *LS*: 12.5 mm, radius of port for *FB*: 20.0 mm. Therefore, the Port Fraction f = 0.2225 and the Exchange Factor F_{i-e} = 0.0156.

Another property that depends on the Reflectance ρ and Multiplicity M for the integrating sphere is its **Radiance** (L). The flux emanating from the surface of the *ISLT* is best described by its Radiance L, defined as the flux density per unit solid angle. It is calculated after multiple reflections as: $L_s = \frac{\Phi_0}{\pi \cdot A_s} \times M$, where the Φ_0 is input light flux. This parameter depends on the sphere radius, reflectance, and port fraction. It can be used to predict the integrating sphere radiance for any given input flux. The ratio $\frac{L_s}{\Phi_0} \times S_{FB}$ is the portion of the light flux that reaches the FB at the exit port A_e area from the input port A_i (*LS*) area after multiple reflections. Here S_{FB} is the actual area of the FB relative to the exit port area A_e. The radiance is calculated as:

$$L_{FB} = \frac{\Phi_0}{\pi \cdot A_s} \times M \times S_{FB} \tag{1}$$

The Multiplicity and Radiance Fraction ($100 \times \frac{L_s}{\Phi_0}$) vs. Reflectance ρ is in the range of $0.900 \rightarrow 0.995$ as shown in Fig. 4.

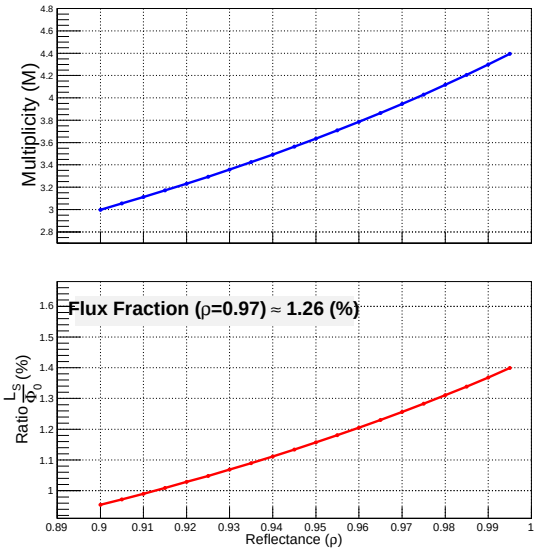

Figure 4: Calculation of Multiplicity and Fraction of Light Flux reaching the FB as a function of the reflectance of the $ISLT$.

If we assume the reflectance of the integrating sphere wall is $\rho = 0.97$, we can see in Fig. 4 that the Multiplicity is ≈ 4 and the Radiance Fraction (Percent of Initial Light Flux that reaches the FB) is $\approx 1.26\%$.

4 Light Transmission for *CALG* and *FTCALG*

A schematic view of the *CALG* is shown in Fig. 5 with a projection of the one side where the FB is installed (blue colored area on the right side). The design of the $FTCALG$ is similar, but with the fiber side radius just a little smaller than the light source side radius. The *MC* studies of the *CALG* and $FTCALG$ were completed for the LED light source in a single position on the face of the light guide. As the LEDs are mounted at a single radial location (see Fig. 1 right), the results are the same for all six LEDs.

The pair of dashed lines, going up and down to the outside of the FB surface (white ring, region 3 in Fig. 5), shown for one LED highlight the angular ranges where direct light from the LED of the LS cannot reach the FB and there is a $dark-region$. An important aspect of the **Light Transmission** is the area of the $dark-region$ surface, which strongly depends on the ratio of the radius of the *CALG* and the FB.

In the simulations for the *CALG* the following dimensions were used:

- Radius of LS = 3.25 mm and FB = 5.00 mm,

- Cylinder Radii = 5.50 mm and 6.00 mm,

For the $FTCALG$ simulations the following dimensions were used:

- Small side radii (touching the FB) = 5.5 mm and 6.0 mm, and large side (touching the LS) = 6.5 mm for both length cases.

For both light guides in the simulations two different lengths were used, 50 mm and 100 mm.

Note that in the simulation the light guide surface is wrapped with a radiant mirror film (VM-2002) and light reflection occurs as on a mirror surface (close to 100% specular reflector). Also, there is a Tedlar film wrapped over the top of the VM-2002 layer for light tightness. Some samples of typical light paths are shown in Fig. 6.

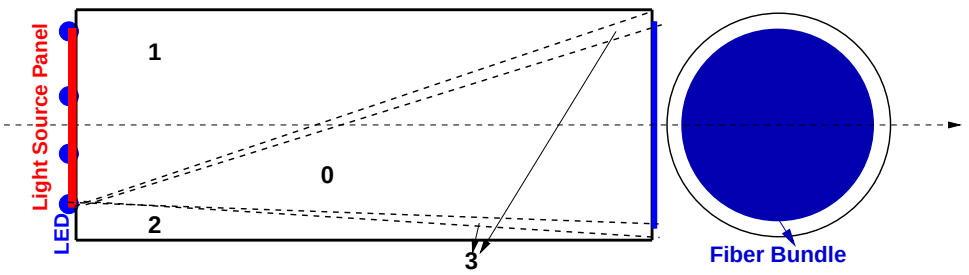

Figure 5: Direct path light flux zones at the end of the light guide where the FB is mounted. The different regions 0, 1, 2, and 3 are defined in the text.

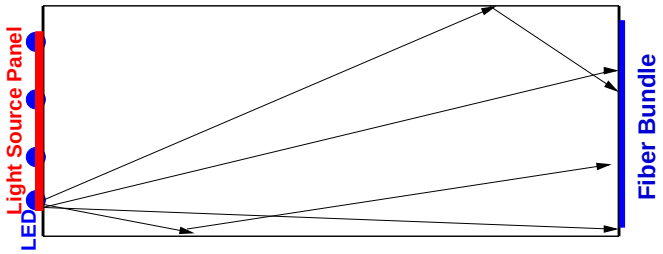

Figure 6: Sample light flux paths within the light guide.

Length (mm)	50		100	
Radius (mm)	5.5	6.0	5.5	6.0
Direct Reach (%)	56.9	56.9	28.6	28.6
Positive Angle (%)	0.4	0.0	14.1	14.1
Negative Angle (%)	28.4	28.3	26.5	22.3
Transmission Efficiency (%)	85.6	85.2	69.3	65.1
Lost in Dark Region (%)	5.7	8.9	2.9	5.7

Table 3: Results of simulation for different lengths are the radii of the *CALG* design.

The results of *MC* simulations for the *CALG* and *FTCALG* cases are shown in Table 3 and Table 4, respectively. Here **Direct Reach** is the light flux fraction that reaches the FB from the *LS* along direct paths where there are no reflections (region 0 in Fig. 5). **Positive Angle** is the fraction of the light flux that reaches the FB after reflections on the upper surface of the light guide (region 1 in Fig. 5) and **Negative Angle** is the corresponding fraction that reaches the FB after reflections on the lower surface of the light guide

(region 2 in Fig. 5). In both tables 0.0% represents the case when light from the *LS* cannot reach to the *FB* in a given region. **Lost in Dark Region** is the light flux lost on the surface of the *dark – region* (region 3 in Fig. 5). In Table 4 the rows labeled **Length** and **Small Radius** are the length and radius of the light guide on the *FB* side for the *FTCALG* design.

Length (mm)	50		100	
Small Radius (mm)	5.5	6.0	5.5	6.0
Direct Reach (%)	56.9	56.9	28.6	28.6
Positive Angle (%)	0.0	0.0	23.6	20.8
Negative Angle (%)	34.3	28.6	39.3	33.7
Transmission Efficiency (%)	91.1	85.4	91.5	83.0
Lost in Dark Region (%)	5.7	8.9	2.9	5.7

Table 4: Results of simulation for different lengths and small radii of the *FTCALG* design.

Tables 3 and 4 show the light guide transmission efficiency for the *CALG* and *FTCALG* designs for both direct and reflected light. Compared to the *ISLT* option they are superior by a factor of ≈40 to 50. The *FTCALG* option is slightly better than the *CALG* option by 5% to 20% depending on the length. The shorter *FTCALG* option (50 mm) with the smaller radius (5.5 mm) is the optimal solution of the design configurations studied.

5 Summary

The *MC* simulation of all cases was done in a plane geometry, but the findings should be applicable for the full 3D representations of the sphere, cylinder, and cone due to the symmetries present. For the case of the *ISLT* compared to the light guide options, the light paths are significantly longer, the light intensity is significantly lower, and the output light pulse is time-slewed at the input to the *FB* due to the long light collection times. Simulations showed for the light guide options that the number of reflections is few and the length paths are short. Also the light intensity lost due to attenuation length effects in the Acrylic materials is negligible given that $\lambda_{Acrylic} \sim 5.5$ m.

- The **Light Transmission** in the *ISLT* theory calculation is:
  1. $\approx$ **1.26%** after **4** reflections.
- The simulations showed that in the *ISLT* case, the **Light Transmission** for 4, 10, and 20 reflections are:
  1. $\approx$ **1.00%** after **4** reflections if accepted $\approx$ **89%** of $\frac{\Phi_r}{\Phi_0}$ ratio,
  2. $\approx$ **2.47%** after **10** reflections if accepted $\approx$ **74%** of $\frac{\Phi_r}{\Phi_0}$ ratio,

3. $\approx$ **4.88%** after **20** reflections if accepted $\approx$ **54%** of $\frac{\Phi_L}{\Phi_0}$ ratio.

- In the *CALG* case:

1. $\approx$ **85.5%** for **50 mm** length and **5.5 mm** or **6.0 mm** radius of the cylinder.

- In the *FTCALG* case:

1. $\approx$ **91.1%** for **50 mm** length and **5.5 mm** small radius of the cone,
2. $\approx$ **91.5%** for **100 mm** length and **5.5 mm** small radius of the cone.

The theoretical calculation and simulation results for the same number of reflections (4) are ≈ 1.26 and $\approx 1.0\%$, respectively, and show very good correspondence.

The simulation showed that for the *CTOF LMS*, the designs using the *CALG* and *FTCALG* are **PREFERABLE** to the *ISLT* design for light transmittance and to maintain the sharp timing of the input light pulse. They also showed that the *FTCALG* design is slightly more effective than the *CALG* design.

Acknowledgments

I am very grateful and many thanks to Daniel Carman, Vitaly Baturin, and Stepan Stepanyan for help, suggestions, recommendations, and corrections in the process of performing this work.